Journal of Biomechanics 176 (2024) 112369

Contents lists available at ScienceDirect

Journal of Biomechanics

journal homepage: www.elsevier.com/locate/jbiomech

Design, implementation and effectiveness of human fascia lata biomechanics for tissue engineering

Lorenza Bonaldi [a], Chiara Giulia Fontanella [b,c,*], Carla Stecco [c,d], Alice Berardo [a,c]

[a] Department of Civil, Environmental and Architectural Engineering, University of Padova, Italy
[b] Department of Industrial Engineering, University of Padova, Italy
[c] Centre for Mechanics of Biological Materials, University of Padova, Italy
[d] Department of Neuroscience, University of Padova, Italy

ARTICLE INFO

Keywords:
Human fascia lata
Mechanical properties
Ex-vivo
Experimental test
Mechanical characterization

ABSTRACT

The fascia lata (FL) is a multi-layered connective tissue with anisotropic mechanical behavior due to its fiber organization. It plays a key role in musculoskeletal functionality, making it important in tissue engineering. Understanding its mechanical response to stimuli like movement or applied pressure is crucial, as the elastic and viscoelastic behavior can vary significantly based on morphological characteristics, harvesting site, and load direction.

Thus, the aim of this review is to summarise through a gap analysis the scientific literature on the biomechanical properties of the human FL, identifying all those features (from the experimental set up to its inherent structural variability) that could affect its biomechanical behaviour, and thus unveiling these emerging correlations. Our research reported key mechanical properties of the FL, such as Young's modulus, Ultimate Tensile Strength, failure strain, and anisotropic response, which are crucial for designing and applying obtained allografts and autografts in soft tissue repair. These insights can help surgeons optimize graft applications—selecting the proper harvesting location, technique, graft type, and suture size—and guide clinicians in rehabilitation for personalized medicine.

1. Background

The fascia lata (FL) is a regular connective tissue, characterized by a multi-layered structure and identified as an aponeurotic deep fascia (Stecco, 2014). It is part of the fascial system with the superficial fascia (Berardo et al., 2024; Stecco and Schleip, 2016), and it gives insertions to many muscular fibers, such as the vastus lateralis and medialis, transmitting the forces in various directions. This precise interaction between FL and the surrounding structures, such as the underlying muscles, guides the collagen fibre orientation inside the FL, introducing anisotropic features (Otsuka et al., 2019, 2018). Among the many functions of FL some authors reported its ectoskeletal role (as a soft tissue skeleton for muscle attachments), its importance for creating compartments for muscles, dissipating stress concentration at entheses, and acting as a protective sheet for underlying structures (Benjamin, 2009; Wood Jones, 1944). For these reasons, the FL has long been of interest to the medical community for its biomechanical and physiological properties, such as thickness and structural stiffness, e.g., that could be indicators related to the increment of pressure in both acute and chronic compartment syndromes (Turnipseed et al., 1995).

In addition, another valuable point that prompted the interest of FL biomechanics has been its growing application to tissue engineering. Its fibrous, sheet-like nature allows the FL to be cut and shaped as required in the surgical procedure (Flanagan and Campbell, 1981). From the 1900s onwards, the FL has been used as a key source of connective tissue for a wide variety of surgical procedures in the field of orthopaedics (Ding et al., 2019; McCarron et al., 2012; Polacek, 2019), plastic surgery ophthalmology (Flanagan and Campbell, 1981; Takahashi et al., 2015), cardiology (Ionescu et al., 1972, 1970; McEnany et al., 1972), thoracic surgery (Molnar et al., 2003) and urology (Brown et al., 2000; Choe et al., 2001; Powell et al., 2004), for a wide variety of applications, including substitution of a torn anterior cruciate ligament (Khiami et al.,

* Corresponding author at: Department of Industrial Engineering, University of Padova, Italy.
E-mail addresses: lorenza.bonaldi@phd.unipd.it (L. Bonaldi), chiaragiulia.fontanella@unipd.it (C.G. Fontanella), carla.stecco@unipd.it (C. Stecco), alice.berardo@unipd.it (A. Berardo).

https://doi.org/10.1016/j.jbiomech.2024.112369
Accepted 13 October 2024
Available online 15 October 2024

2013). Recently, human FL has been also considered for novel applications such as Critical Size Bone Defect (CSBD) treatments, demonstrating its potential use as a periosteal-like scaffold (Manon et al., 2022).

However, some works reported the need to improve graft preparation techniques to minimize differences and increase the repeatability (Ferro et al., 2015). Indeed, many factors usually contribute to the success or failure of an autograft / allograft reconstruction, including grafting preparation at the time of surgery, graft fixation, and, especially, the biomechanical suitability of the implant with the anatomical site of the application. This being the case, experimental values such as Ultimate Tensile Strength (UTS), Young's (or Elastic) modulus (E) and maximum tissue strain before breakage may represent preliminary indicators of a graft successful performance *in vivo*, thus highlighting the fundamental clinical importance of a clear and reliable investigation of the FL biomechanics also for rehabilitative interventions.

Since the beginning of the XX century, some studies have been performed to characterize the elastic and viscoelastic properties of human FL when subjected to external stimuli, to simulate its biomechanical function under tensile loads, as for example (Bonaldi et al., 2023a, 2023b; Gratz, 1931; Otsuka et al., 2018). However, from a careful analysis of the available literature, it is clear that FL mechanical response significantly depends on many variables, such as different sample harvesting and preparation, mechanical test parameters, direction of the fibres with respect to the applied load, confirming among the others its anisotropic asset and site-dependent characteristics (de Campos Azevedo et al., 2021).

Therefore, the aim of the present study was to summarise the scientific literature on the biomechanical properties of the human FL and related testing protocols, in order to correlate them with the tissue microstructural configuration. A clear identification of possible biases that could lead to a misleading of the results would help during test planning and applications, to not compromising their efficiency. This review has been focused on the tensile behaviour of human FL, from sample harvesting and experimental setup to mechanical properties. These insights could be useful to surgeons during daily practice in planning fascia orientation (Chaudhry et al., 2007), selecting graft location, applicative technique, and graft type based on site properties (de Campos Azevedo et al., 2021), and determining the correct size of the suture to be used in the operative procedure (Gratz, 1931).

2. Methods

2.1. Search strategy and criteria

The results of this review were reported on the basis of the Preferred Reporting Items for Systematic reviews and Meta-Analyses (PRISMA) guidelines. Using database-specific subject headings, SCIENCEDIRECT and PUBMED were searched from inception until March 2024. Search terms were included queries with combination of the following keywords: ("fascia lata" OR "iliotibial band") AND ("uniaxial tensile test" OR "stress relaxation test" OR "mechanical properties" OR "constitutive parameters" OR "dynamic loading" OR "cyclic behaviour"). In total 217 articles from databases and 6 articles from other sources were included (Fig. 1). PICO framework helped in developing studies evaluation:

P (population/problem): biomechanical properties of specimens from human donors FL (inclusive of the iliotibial band);
I (intervention or exposure): uniaxial tensile test;
C (comparison): specimen preparation, storage, experimental setup and protocol, outcomes analysis and evaluation;
O (outcome): stiffness, Young's modulus, stress–strain at failure, viscosity.

Some articles were removed (e.g., duplicates), and remaining articles have been fully revised (192). Articles were included if they described topics in accordance with PICO description or if they reported any relevant discussion. Finally, 32 articles were considered eligible for the comparative analysis. Three other expert reviewers (two engineers and

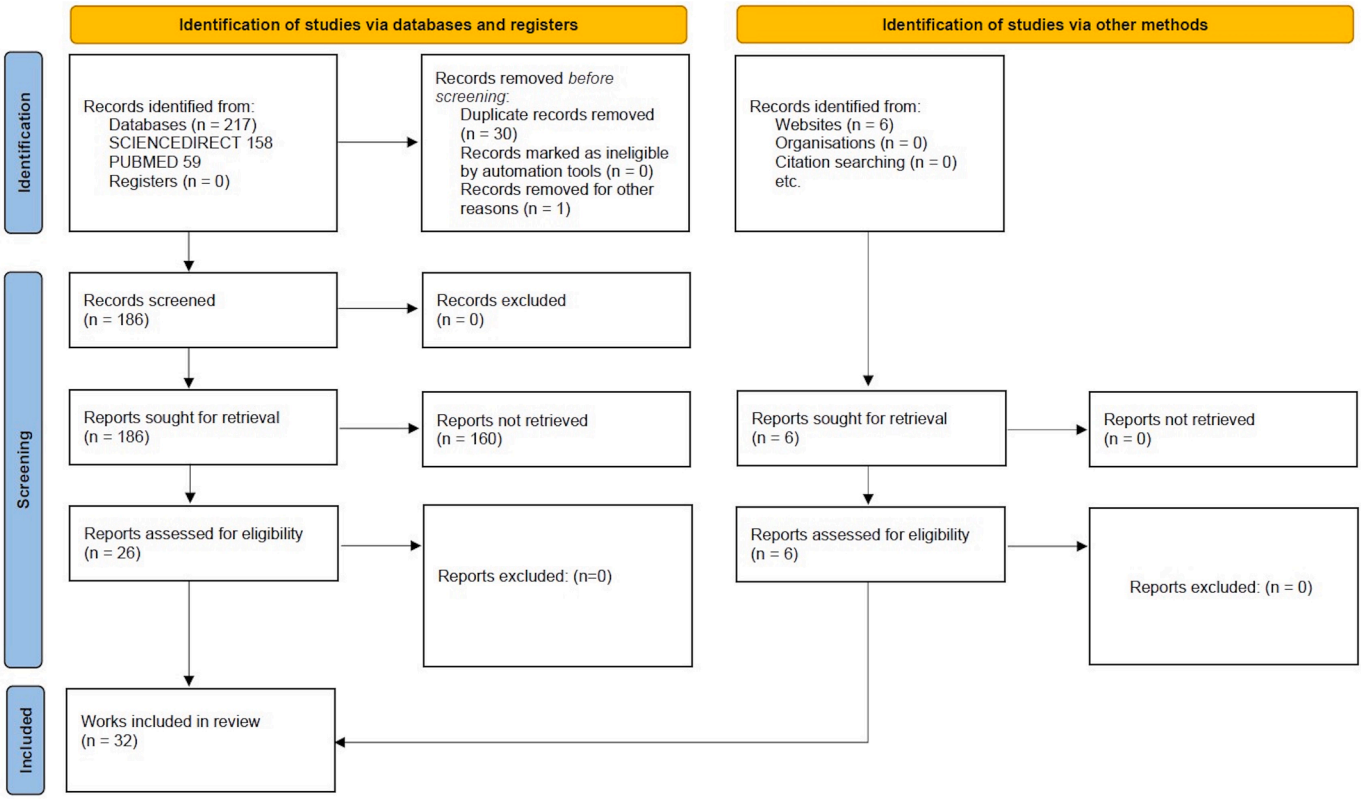

Fig. 1. PRISMA flow diagram.

one clinician) supervised the selection and supplemented this review with additional elements and observations. This review focused on mechanical testing and characterization of human FL, considering also additional mechanical tests compared to uniaxial tests, e.g., biaxial tests.

3. Results

3.1. Design of the mechanical test

3.1.1. Micro and macrostructure of fascia lata

The correspondence between fascia microstructural configuration and its biomechanical behaviour can be considered the first key factor for FL evaluation through mechanical tests. The FL is an aponeurotic fascia, formed by two–three layers of fibrous connective tissue (Benetazzo et al., 2011; Stecco et al., 2008), divided by thin layers of loose connective tissue, rich in hyaluronan which is responsible for loose connective tissue viscosity (Stecco et al., 2023; Stecco, 2014). According to the characterization of the literature, in general, the 2–3 layers of dense connective tissue have a thickness of 277 μm ± 86 μm each and are separated by layers of loose connective tissue of 43 μm ± 12 μm each, which lead to an average total thickness of 944 μm ± 156 μm (Stecco, 2014). The fibrotic component plays a role in the force transmission, while the loose connective tissue guarantees the gliding between the various fibrous layers and between fascia and the underlying muscles (Stecco, 2014).

The FL can be divided into different parts according to its position relative to the underlying muscles (Platzer et al., 2014; Stecco, 2014). The posterior portion covers the ischiocrural muscles and proximally is in continuity with the gluteal muscles. The lateral portion is the thicker one because it is reinforced by the iliotibial tract (ITT). It is important to note that some last researchers (Stecco et al., 2013; Stecco, 2014) highlighted that the ITT is not an isolated structure, but it is totally embedded into the FL. In such a way, as underlined by (Benjamin, 2009) "the ITT is part of a whole fascial stocking completely encircling the thigh, is extensively connected to the lateral intermuscular septum". The anterior portion covers the quadriceps muscle and the sartorius one, whilst the medial portion covers the adductors muscles (Benjamin, 2009; Platzer et al., 2014; Stecco, 2014).

The biomechanics of the fascial tissues is therefore influenced by the elements mentioned above (such as the loose connective tissue and the close relationship with the muscles through the myofascial expansions), but it is especially a function of the arrangement of the fibres (mainly collagen, more numerous than the elastic fibres (Pirri et al., 2022)). Indeed, the myofascial expansions could be considered as fibrous extensions originating from the muscle and continuing beyond the muscle itself, into the fascia (A. Stecco et al., 2009). The spatial orientation of collagen fibres varies from layer to layer, in each layer the collagen fibres run parallel in a specific direction (as also reported by (Szotek et al., 2012)), while commonly the directions of the fibres between the layers form an angle of 75°-80° (Stecco, 2014). This arrangement leads to the ability of the fascial system to resist tensile loads along with peculiar directions (Stecco, 2014), as also observed for the crural fascia (C. Stecco et al., 2009).

3.1.2. Sample collection

Samples from cadavers or even excised during surgery (e.g., (Gratz, 1931)) often come from elder subjects (> 60 y/o), however some studies reported case studies also from younger donors even if the sample size appears to be quite limited (early-young (<18) and young (18–40) population)(Aurora et al., 2011; Balsly et al., 2008; Butler et al., 1984; Caplan and Kader, 2014; Derwin et al., 2008; Erivan et al., 2018; Gratz, 1931; Hammer et al., 2012; Zwirner et al., 2019). An aspect that randomly depends on sample availability is the donor's sex: a clear majority of male donors are reported, with few exceptions (Bonaldi et al., 2023a; Manon et al., 2022; Otsuka et al., 2018). Another variable that represents a key information is the harvesting site: in many works, unfortunately this detail has been omitted, but (Otsuka et al., 2018) reported differences in the mechanical response of FL from anterior, posterior, medial and lateral legs sites. Moreover, since the FL has been observed to be a highly anisotropic and composite material (Butler et al., 1984), when dealing with its mechanical characterization, affecting parameters are the fibres directions of both layers and thus how the specimen has been cut with respect to them. It has been proved that fibres influence the mechanical properties when they are oriented parallel or perpendicular to the applied load (Otsuka et al., 2018; C. Stecco et al., 2009), thus results may be wrongly interpreted if the reference of fibres direction, when cutting the sample, is missing. We noticed this aspect to be highlighted in some of the analysed works, even though the aim of some of those studies then focused on other aspects (Aurora et al., 2011; Balsly et al., 2008; Butler et al., 1984; de Campos Azevedo et al., 2021; Derwin et al., 2008; Hammer et al., 2012; Steinke et al., 2012).

3.1.3. Sample conservation

Storage, thawing and hydration may alter the mechanical performances of biological materials as well. When comparing the available protocols for FL before testing, these collateral procedures have been also reported. Fresh samples should be the first choice when available (to be tested within 72 h) (Crawford, 1969; de Campos Azevedo et al., 2021; Gratz, 1931; Thomas et al., 1998), even if the most common solution among the authors resulted in fresh-frozen (−20 °C to −85 °C) specimens (Bonaldi et al., 2023a; Butler et al., 1984; de Campos Azevedo et al., 2021; Derwin et al., 2008; Erivan et al., 2018; Hammer et al., 2012; Steinke et al., 2012; Zwirner et al., 2019), sometimes with a precooling before freezing (Erivan et al., 2018; Hammer et al., 2012; Steinke et al., 2012; Zwirner et al., 2019). Indeed, it has been reported that freezing the samples for a short time (i.e., 5 min) before cutting demonstrated to prevent slippage between layers (Crawford, 1969). In addition, some works tested also some previously processed samples (see Table 1), with evidence that these processes could alter the tissue properties, as ice formation that potentially weaken the collagen microstructure of the FL (Lemer et al., 1999).

Another issue during mechanical tests is sample dehydration, which consistently changes the response of the material. The reduction of water content in time and consequent sample drying could influence the microscale, with macroscopic effects such as an increase in material stiffness and a reduction of material elongation (brittle behaviour). For these reasons, authors have suggested possible solutions, to avoid material alterations before and during the mechanical tests. In some works (Balsly et al., 2008; de Campos Azevedo et al., 2021; Derwin et al., 2008; Gratz, 1931; Kubricht et al., 2001; Lemer et al., 1999), authors suggested keeping the samples plunged into the saline solution, e.g., Phosphate Buffered Saline (PBS) solution, and immediately testing them when removed. Moreover, especially when the mechanical test duration exceeds tens of minutes, others (Bonaldi et al., 2023a; Butler et al., 1984; de Campos Azevedo et al., 2021; Hammer et al., 2012; Otsuka et al., 2020) continued pipetting the samples with alcohol or saline solution for the entire test duration, while others (Aurora et al., 2011; Derwin et al., 2008) kept the samples in saline bath.

3.1.4. Sample preparation

Among the analysed literature, a wide variability has been noticed about the specimen cut and shape after removal from the donor (Fig. 2). Results are usually normalized by sample length and cross-sectional area (as reported in the following), thus sample shape and size should not influence the results. However, these details help in understanding the sample availability and measure repeatability, especially when other quantities, like stiffness or maximum force, are reported. Authors from (Choe et al., 2001; Dwyer and Kreder, 2008; Polacek, 2019) referred to surgical protocols guides with reference to graft dimensions/shape/fibres orientations. Additional information as the sample cutting into a specific shape (i.e., dog-bone shape, (Zwirner et al., 2019), dumbbell (Balsly et al., 2008)) or the removal of other close tissues (i.e., adipose tissue) (Balsly

Table 1
Specimen harvesting, conservation and protocol as reported within the analysed works. If details were not within the manuscripts, the reference was omitted.

Sample collection		
Donors	Equal gender distribution	(Bonaldi et al., 2023c; Manon et al., 2022; Otsuka et al., 2018; Steinke et al., 2012)
	<60 y/o	(Aurora et al., 2011; Balsly et al., 2008; Butler et al., 1984; Caplan and Kader, 2014; Derwin et al., 2008; Erivan et al., 2018; Gratz, 1931; Hammer et al., 2012; Wytrykowski et al., 2016; Zwirner et al., 2019)
Sample size	Single subject	(Choe et al., 2001; Crawford, 1969; Thomas et al., 1998)
	Multiple subjects with specified number of legs	(de Campos Azevedo et al., 2021; Otsuka et al., 2020, 2018)
Tissue quality	Alterations (if reported, e.g., long term steroids)	(Thomas et al., 1998)
	No alterations (if specified)	(Balsly et al., 2008; Birnbaum et al., 2004; Bonaldi et al., 2023c; Butler et al., 1984; de Campos Azevedo et al., 2021; Derwin et al., 2008; Ferro et al., 2015; Otsuka et al., 2018, 2020; Taylan et al., 2022; Wytrykowski et al., 2016)
Body harvesting	Specified harvesting site (with reference to the body anatomy)	(Aurora et al., 2011; Balsly et al., 2008; Butler et al., 1984; de Campos Azevedo et al., 2021; Derwin et al., 2008; Hammer et al., 2012; Manon et al., 2022; Otsuka et al., 2020, 2018; Smeets et al., 2017; Steinke et al., 2012; Taylan et al., 2022; Wytrykowski et al., 2016; Zwirner et al., 2019)
Sample conservation		
Hydration	Before testing (Saline solution immersion e.g., PBS)	(Balsly et al., 2008; Bonaldi et al., 2023c; Gratz, 1931; Hammer et al., 2012; Kubricht et al., 2001; Lemer et al., 1999; Gordon et al., 2017; Milks et al., 2018)
	During testing (pipetting/bath)	(Aurora et al., 2011; Bonaldi et al., 2023c; Butler et al., 1984; de Campos Azevedo et al., 2021; Derwin et al., 2008; Ferro et al., 2015; Gratz, 1931; Hammer et al., 2012; Otsuka et al., 2018, 2020; Smeets et al., 2017; Steinke et al., 2012)
Treatments	Irradiation/freeze drying/fixation (e.g., formaldehyde)/solvent-dehydrated	(Aurora et al., 2011; Balsly et al., 2008; Choe et al., 2001; Crawford, 1969; Derwin et al., 2008; Erivan et al., 2018; Kubricht et al., 2001; Lemer et al., 1999; Otsuka et al., 2020, 2018; Steinke et al., 2012)
Freezing	Temperature (−20 °C, −30 °C, −80 °C, −85 °C)	(Bonaldi et al., 2023c; Butler et al., 1984; Derwin et al., 2008; Erivan et al., 2018; Hammer et al., 2012; Smeets et al., 2017; Steinke et al., 2012; Taylan et al., 2022; Wytrykowski et al., 2016; Zwirner et al., 2019; Gordon et al., 2017)
	Precooling before freezing	(Erivan et al., 2018; Hammer et al., 2012; Steinke et al., 2012; Zwirner et al., 2019)
	More freezing cycles	(Derwin et al., 2008)
Thawing and testing	Within 72 h after death/harvesting	(Crawford, 1969; de Campos Azevedo et al., 2021; Gratz, 1931; Thomas et al., 1998)
	Testing immediately after thawing	(Erivan et al., 2018)
Sample preparation		
Specific shape	Dog-bone	(Smeets et al., 2017; Zwirner et al., 2019)
	Dumbbell	(Balsly et al., 2008)
	Adipose tissue removal	(Balsly et al., 2008; Ferro et al., 2015; Hammer et al., 2012; Otsuka et al., 2020, 2018; Taylan et al., 2022)
Reference to specific protocol guides	Sling	(Dwyer and Kreder, 2008)
	Capsular (upper limb) reconstructions	(Polacek, 2019)
	Labral (hip) reconstruction	(Ferro et al., 2015)
	Suburethral patch	(Choe et al., 2001)
Measurements	Multiple measurements (e.g., different operators or different points of measure)	(Bonaldi et al., 2023c; Butler et al., 1984; Choe et al., 2001; de Campos Azevedo et al., 2021; Derwin et al., 2008; Otsuka et al., 2018, 2020; Smeets et al., 2017; Gordon et al., 2017)
	Digital Image Analysis / digital calliper	(Bonaldi et al., 2023c; de Campos Azevedo et al., 2021; Ferro et al., 2015; Otsuka et al., 2018, 2020; Smeets et al., 2017; Steinke et al., 2012; Taylan et al., 2022)
	Initial preload	(de Campos Azevedo et al., 2021; Ferro et al., 2015; Gordon et al., 2017; Wytrykowski et al., 2016)
Experimental setup		
Specific grips and anchoring solutions	Sandpaper	(de Campos Azevedo et al., 2021; Ferro et al., 2015; Otsuka et al., 2020, 2018; Smeets et al., 2017)
	Resin	(Caplan and Kader, 2014; Hammer et al., 2012; Steinke et al., 2012)
	Aluminum strips	(Thomas et al., 1998)
	Glue	(Otsuka et al., 2020, 2018)
	roughened surface clamps	(Gordon et al., 2017)
	3D-printed clamps	(Taylan et al., 2022; Zwirner et al., 2019)
	Other solutions	(Balsly et al., 2008; Bonaldi et al., 2023c; Butler et al., 1984; Derwin et al., 2008; Ferro et al., 2015; Lemer et al., 1999; Manon et al., 2022; Smeets et al., 2017)
Other considerations	Balance of the gripping force to not alter tissue	(Caplan and Kader, 2014; Erivan et al., 2018)
	Marking the sample near grip to evaluate slippage (e.g. with pins)	(Butler et al., 1984)
	Top-bottom fixation performed in sequence to align specimens due to gravity	(Erivan et al., 2018; Gordon et al., 2017)

et al., 2008; Hammer et al., 2012; Otsuka et al., 2020, 2018) provided the reader with a full procedure description. When cutting the specimens for the tests, some works referred also to fibres directions (Bonaldi et al., 2023a; Derwin et al., 2008; Szotek et al., 2012). One difficult quantity to measure before testing could be the FL sample thickness. For this reason, some authors proposed the use of a digital calliper (Bonaldi et al., 2023a; de Campos Azevedo et al., 2021; Otsuka et al., 2020, 2018) or eventually the Digital Image analysis (Hammer et al., 2012; Taylan et al., 2022) to evaluate the thickness of the samples.

3.1.5. *Experimental setup*

Last but not least, also the machine setup for mechanical tests could affect the final results. FL is a slippery tissue due to its constitution and multilayer organization (Stecco, 2014). During tensile testing slippage could happen, leading to an underestimation of the material response to the applied stimulus. This being the case, many authors experimented and then suggested valuable solutions to avoid this difficulty. Sandpaper (de Campos Azevedo et al., 2021; Otsuka et al., 2020, 2018) or resin fixation (Caplan and Kader, 2014; Hammer et al., 2012; Steinke et al.,

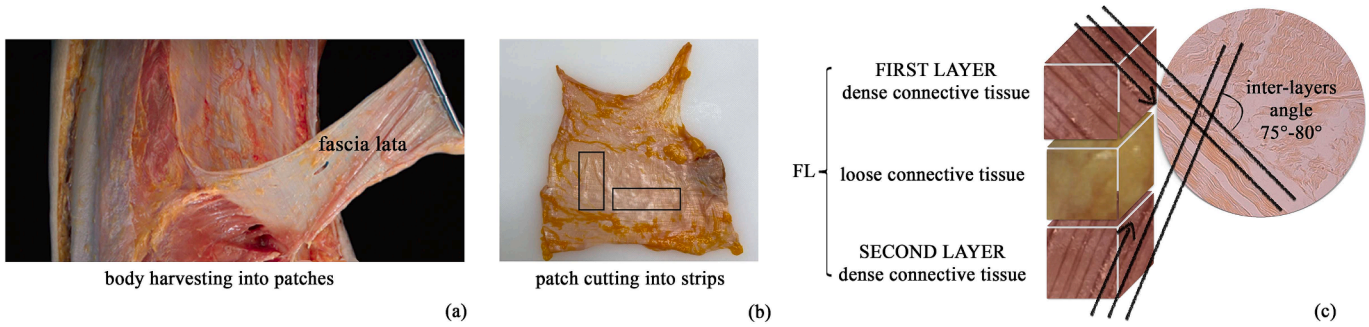

Fig. 2. (a) Cadaveric study: FL is detached from the quadriceps muscle and lifted medially. FL is easily separated from the underlying muscle due to the loose connective tissue (image taken from (Stecco, 2014)). (b) FL patch with indication of cutting strips (image taken from (Bonaldi et al., 2023a)). (c) Microstructure of FL: 2 layers of dense connective tissue separated by a layer of loose connective tissue. The directions of the fibres between the layers form an angle of 75°-80°.

2012) appeared to be the most adopted alternatives, combined or substituted by aluminium strips (Thomas et al., 1998), with glue (Otsuka et al., 2020, 2018) or available customized techniques e.g., roughened surface clamps (Gordon et al., 2017), 3D-printed clamps (Taylan et al., 2022; Zwirner et al., 2019), gripping system reinforced with heavy steel clamps (Lemer et al., 1999) or others, (Balsly et al., 2008; Butler et al., 1984; Derwin et al., 2008). (Butler et al., 1984) also suggested marking the samples near the grips, to evaluate any slippage, while (Ferro et al., 2015) used galvanized wire. An efficient sample fixation to the machine grips could prevent the specimen also from possible unexpected stresses, alterations, and damage.

3.2. Implementation of mechanical testing

In the following section, an overview of the studies which have characterized the mechanical properties of human FL by mainly performing uniaxial tensile tests have been collected, compared, and discussed. Also preconditioning procedures have been included as a fundamental step prior to tensile tests, since in biological tissue as FL it contributes to a preliminary collagen fibre reorganization (Cheng et al., 2009; Ebrahimi et al., 2019). Indeed, when crimped collagen fibres become straightened, the tissue tensile response stabilizes, for more repeatable and consistent results (Bonaldi et al., 2023a).

3.2.1. Preconditioning

When dealing with biological materials, preconditioning has been observed to provide a first loading history to the specimen with repeatable and comparable subsequent testing results, thus reducing experimental variability (Cheng et al., 2009; Ebrahimi et al., 2019). In particular, it causes microstructural changes as collagen fibres re-align along the same direction as one of the ensuing mechanical tests. However, to test human FL, preconditioning appears to be not a common practice, and, in addition, it showed a protocol variability. In some works, the reported assumption was to address the first tensile curve (Otsuka et al., 2018) or the first two loading–unloading cycles (de Campos Azevedo et al., 2021; Otsuka et al., 2020) as sample preloading, since they differed from the other curves (with stiffness 17.5–25.5 % lower (de Campos Azevedo et al., 2021)). The majority of the works adopted n cycles of loading–unloading, and the most frequent choice was a sequence of 10 cycles with fixed applied maximum strain as sample preloading (Aurora et al., 2011; Bonaldi et al., 2023a; Gordon et al., 2017; Hammer et al., 2012; Manon et al., 2022; Smeets et al., 2017), even if also $n = 5$ (Balsly et al., 2008; Derwin et al., 2008), 7 (Steinke et al., 2012), up to even 20 (Taylan et al., 2022; Zwirner et al., 2019) were also observed. Maximum elongation strain has been set within the range of 0–7 % of the initial specimen length adopting a strain rate from 0.1 %/s to 10 %/s (Table 2). The number of loading–unloading cycles and the strain rate should be set depending on the viscoelasticity of the tested material, in order also to minimize the energy dissipated in one cycle and thus allow repeatable measurements, which is improved by adjusting the preconditioning protocol with a high number of repetitions and a relatively high strain level (Ebrahimi et al., 2019).

3.2.2. Tensile tests and mechanical properties

An uniaxial tensile test is usually performed by applying a controlled displacement to the sample in a single tensile direction, where the force is measured from the sensor i.e., the load cell. As a common practice, the imposed displacement and the recorded force are usually converted into the engineered strain ε and the nominal stress σ, as follows:

$$\varepsilon = \frac{l - l_0}{l_0}$$

$$\sigma = \frac{F}{A}$$

The engineering strain is the length variation of the specimen in the direction of the applied displacement, with respect to the gauge length (l_0), while the nominal stress is the measured force normalized by the cross-sectional area of the specimen. These two quantities are not affected by the sample dimensions and are usually plotted one with respect to the other in the so-called stress–strain curve (Fig. 3d), for a direct comparison with results obtained from different authors. An additional (indirect) mechanical quantity that describes the elastic response of materials is the elastic modulus or Young's modulus (E), defined as the ratio between the stress and the associated strain. For an almost linear stress–strain curve, E represents the slope of that curve. Biological materials such as the FL are usually strongly non-linear (Bonaldi et al., 2023a; Singh and Chanda, 2021), thus E is a value which usually describes a portion of the stress–strain, the linear region (Fig. 3d, orange region) and in particular the region that appears almost linear (i.e., the slope of the stress–strain curve in the linear region as part of body physiological working range):

$$E = \frac{\Delta\sigma}{\Delta\varepsilon}$$

However, especially when referring to older works, maximum force measured, maximum displacement and material stiffness (i.e., the slope of the force–displacement curve) were reported instead, as for example (Caplan and Kader, 2014; Gratz, 1931; Thomas et al., 1998). The stiffness (N/mm) is related to E with respect to the specimen initial length and the cross-sectional area:

$$k = \frac{F}{\Delta l} = \frac{AE}{l_0}$$

To be thorough, these results were also included (Table 2) but not compared among the others.

From uniaxial tensile tests the relationship between the stress and the strain in FL, with reference to the strain rate adopted during the

Table 2
Mechanical properties of human FL and protocols by different authors. Colors refer to the reported quantity for each analyzed work.

Authors	Including the influence of:					Type of test	Preconditioning	Results				
	Gender (n°)	Conservation	Sample shape	Site	Loading directions (Longitudinal of trasverse with respect to fibers directions)		no of cycles of loading–unloading (strain rate)	strain rate (%/s) velocity (mm/s)	Elastic Modulus (MPa) (strain interval)	Stiffness (N/mm) (strain interval)	UTS (MPa) Max Force (N)	Strain at break (%) Max displacement (mm)
Aurora, A. et al. 2011	N/A (30)	Decellularized, lyophilized, PLLA reinforced	50 × 50 mm	Iliotibial tract	Longitudinal	Biaxial	10 (0.1 mm/s)	0.5	N/A	22 ± 2	315 ± 23	16.2 ± 2
		Decellularized, lyophilized, PLLA/PGA reinforced								27 ± 4	415 ± 51	18.6 ± 2.9
Balsly, C. L. et al. 2008	N/A	freeze-dried	Dumbbell	Lateral thigh	Longitudinal	Uniaxial	5 (1 %/s)	10	371.9 ± 99.8	N/A	93.4 ± 28.2	N/A
		18.3–21.8 kGy irradiation							366.27 ± 87.4		97.3 ± 17.1	
		24.0–28.5 kGy irradiation							238.5 ± 113.4		70.9 ± 19.0	
Birnbaum, K. et al. 2004	N/A (6)	Fresh	N/A	Iliotibial tract	N/A	Uniaxial	N/A	N/A	N/A	17	860	65
Bonaldi L. et al. 2023	Female (2) & Male (2)	Fresh-frozen	30 × 4 mm	Lateral thigh	Longitudinal, along layer 1	Uniaxial	10 (1 %/s)	0.5	102.2 ± 60.6	N/A	6.3 ± 4.1	14 ± 4
					Transverse along layer 1				8.0 ± 3.6		0.9 ± 0.4	16 ± 11
					Longitudinal, along layer 2				12.7 ± 11.4		1.3 ± 0.8	18 ± 6
					Transverse, along layer 2				67.0 ± 65.2		6.6 ± 3.1	19 ± 7
Choe, J. M. et al. 2001	N/A (1)	freeze-dried, gamma- irradiated	Full strip sling 20 × 50 mm	N/A	N/A	Uniaxial	N/A	0.08	N/A	N/A	217 ± 66	1.36 ± 0.78
			Patch suture sling 20 × 50 mm								58 ± 22	31.5 ± 3.49
Crawford, J. S. 1969	N/A (1)	Fresh	Rectangular	N/A	Longitudinal	Uniaxial	N/A	N/A	N/A	N/A	31.9 ± 17.6	15
		Irradiated									29.8 ± 13.5	
de Campos Azevedo, C. I. et al. 2021	Female (4) & Male (6)	Fresh	Graft (6-layered thrice-folded)	Lateral proximal thigh	Longitudinal	Uniaxial	2	0.5	32.9 ± 19.6	489.0 ± 267.8	N/A	N/A
				Lateral mid-thigh					44.0 ± 31.3	562.4 ± 294.8		
Derwin, K. A. et al. 2008	N/A (10)	Fresh-frozen	12 × 45 mm	Iliotibial tract	Longitudinal	Uniaxial	5	0.17	389 ± 189 (2–5 %)	85.1 ± 15.4 (4.5–5.5 %)	N/A	N/A
		Antibiotic soak treatment							532 ± 106 (2–5 %)	98.2 ± 16.2 (4.5–5.5 %)		
		Accellularized + antibiotic soak treatment							440 ± 326 (2–5 %)	71.2 ± 38.9 (4.5–5.5 %)		
Erivan, R. et al. 2018	Female (2) & Male (5)	Cryopreservation	30 × 10 mm	N/A	N/A	Uniaxial	N/A	0.17	319.7 ± 206.9	N/A	26.2 ± 14.5	16.9 ± 11.2

(*continued on next page*)

Table 2 (*continued*)

Authors	Including the influence of:					Type of test	Preconditioning	Results			
	Gender (n°)	Conservation	Sample shape	Site	Loading directions (Longitudinal of trasverse with respect to fibers directions)		no of cycles of loading–unloading (strain rate)	strain rate (%/s) velocity (mm/s)	Elastic Modulus (MPa) (strain interval)	Stiffness (N/mm) (strain interval)	UTS (MPa) Max Force (N)	Strain at break (%) Max displacement (mm)
Hammer, N. et al. 2012	Female (2) & Male (8)	Fresh-frozen	170 × 15 mm	Iliotibial tract	Longitudinal	Uniaxial	10	N/A	335.47 ± 101.9 (4–11 %)	N/A	35.8 ± 16.4	10.3 ± 5.4
Lemer, M. L. et al. 1999	N/A	Solvent dehydrated	Rectangular	N/A	N/A	Uniaxial	N/A	100	N/A	114.5 ± 11.8	319 ± 34	N/A
		Freeze-dried								89.2 ± 9.5	250 ± 29	
Manon et al. 2022	Female (3) & Male (3)	Frozen	Rectangular, 2 × 5 cm	Median to lateral lip of the linea aspera including iliotibial tract	Longitudinal	Uniaxial	10 (0.25 mm/s)	0.25	1533.6 ± 0.4	N/A	96.8 ± 3.2	N/A
								0.5	1545 ± 55.0	N/A	N/A	
Otsuka, S. et al. 2018	Male (6)	Formaline-fixed	Square (40 × 40 mm)	Anterior	Longitudinal	Uniaxial	1	0.42	264.3 ± 90.3	109.6 ± 40.9	N/A	N/A
					Transverse				33.2 ± 16.5	13.3 ± 6.4		
				Lateral	Longitudinal				289.9 ± 109.1	279.0 ± 61.1		
					Transverse				2.8 ± 2.4	2.6 ± 2.1		
				Medial	Longitudinal				81.4 ± 36.1	24.1 ± 9.1		
					Transverse				20.0 ± 15.5	4.8 ± 2.5		
				Posterior	Longitudinal				135.2 ± 71.2	39.7 ± 18.8		
					Transverse				41.9 ± 13.2	12.6 ± 4.0		
	Female (6)			Anterior	Longitudinal				166.3 ± 94.7	55.6 ± 24.3		
					Transverse				54.1 ± 34.1	17.8 ± 7.9		
				Lateral	Longitudinal				260.2 ± 41.3	286.9 ± 49.3		
					Transverse				3.6 ± 2.2	3.2 ± 1.4		
				Medial	Longitudinal				60.6 ± 23.5	14.9 ± 6.5		
					Transverse				45.4 ± 22.6	11.1 ± 5.7		
				Posterior	Longitudinal				76.9 ± 36.7	27.1 ± 15.7		
					Transverse				22.2 ± 12.6	7.7 ± 4.8		
Otsuka, S. et al. 2020	Male (12)	Formaline-fixed	40 × 20 mm	Proximal	Longitudinal	Uniaxial	N/A	0.42	site 1 337.9 ± 103.3 site 2 362.7 ± 50.5	N/A	N/A	N/A
			30 × 10 mm	Distal					site 3 219.4 ± 68.8 site 4 113.4 ± 63.7 site 5 130.4 ± 73.7			
Smeets, K. et al. 2017	N/A (11)	Fresh-frozen	Dog-bone (100 × 20 mm)	Iliotibial tract	N/A	Uniaxial	10 (0.1 %/s)	2	610 ± 171	N/A	75 ± 11.8	17.6 ± 4.8
Steinke, H. et al. 2012	Female (6) & Male (7)	Fresh-frozen	Rectangular	Iliotibial tract	Longitudinal	Uniaxial	7	0.42	564.7 ± 193.8 (4–11 %)	N/A	N/A	N/A
		Ethanol-fixed							951.4 ± 383.6 (4–11 %)			

(*continued on next page*)

Table 2 (*continued*)

Authors	Including the influence of:					Type of test	Preconditioning	Results				
	Gender (n°)	Conservation	Sample shape	Site	Loading directions (Longitudinal of trasverse with respect to fibers directions)		no of cycles of loading–unloading (strain rate)	strain rate (%/s) velocity (mm/s)	Elastic Modulus (MPa) (strain interval)	Stiffness (N/mm) (strain interval)	UTS (MPa) Max Force (N)	Strain at break (%) Max displacement (mm)
		Ethanol-rinsed							555.4 ± 201.3 (4–11 %)			
		Formaline-fixed							675.3 ± 150.9 (4–11 %)			
		Formaline-rinsed							630.5 ± 117.8 (4–11 %)			
Thomas, O. L. et al. 1998	M (1)	Fresh	Tubulized	N/A	N/A	Uniaxial	N/A	N/A	N/A	6.2 ± 1.06	35.7 ± 14.1	3.5 ± 0.2
			Rectangular							3.3 ± 0.58	N/A	4.8 ± 0.5
Voskerician, G. et al. 2009	N/A	N/A	10 × 55 mm	N/A	Longitudinal Transverse	Uniaxial	1 (0.17 mm/s)	8.33	N/A	N/A	30 5	< 15
Zwirner, J. et al. 2019	Female & Male (33)	Fresh-frozen	Dog-bone (60 × 12 mm)	Iliotibial tract	N/A	Uniaxial	20	0.33	408 ± 232	N/A	29 ± 17	15 ± 5
	Female (10)								502 ± 284		35 ± 22	13 ± 5
	Male (23)								366 ± 198		26 ± 13	15 ± 4

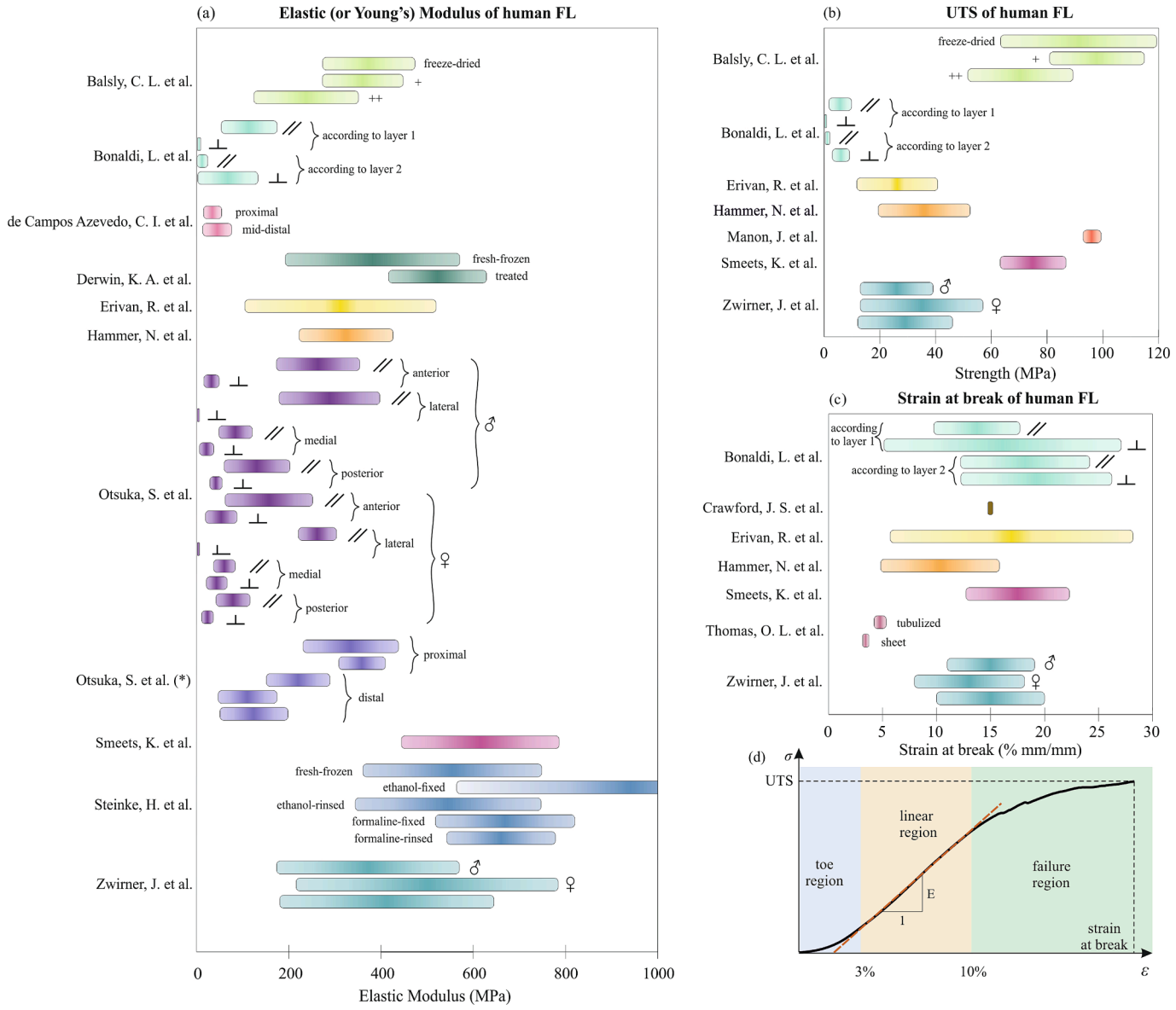

Fig. 3. Mean and standard deviation (when reported) of the mechanical properties of human FL among the authors. (a) Elastic (or Young's) modulus, E; (b) uniaxial tensile strength (UTS); (c) strain at break; (d) an example of a stress–strain curve from an uniaxial tensile test of human FL. UTS and strain at break are identified when the breakage occurs, while E corresponds to the slope of the curve in the linear region. Legend of symbols: "+" and "++" stand for mechanical properties of FL allografts, irradiated on dry ice at a low absorbed dose (18.3–21.8 kGy) and a moderate absorbed dose (24.0–28.5 kGy), respectively. "⊥" and "//" refer to experimental tests performed perpendicular or parallel to fibers directions, respectively. "♀" or "♂" identify tests realized on female or male groups, respectively. "*" refers to the work of Otsuka et al. 2020.

tests, can be observed (in both its linear or non-linear intervals), in order to quantify mechanical parameters such as the maximum strain, the strength and the elastic modulus. Due to the viscoelastic behaviour which characterizes the biological tissues, the adopted strain rate usually plays a significant role in the final tests output, with a considerable increase in both the strength and *E*, and a consequent reduction in the maximum strain, when increasing the strain rate. For example, as reported in Table 2, if considering fresh-frozen donors, Bonaldi et al. (Bonaldi et al., 2023a) implemented a uniaxial tensile test with a strain rate of 0.5 %/s, lower than Smeets et al. (Smeets et al., 2017), who adopted 2 %/s. When comparing the elastic modulus, it can be evinced that a higher value (six times) can be obtained with an incremental strain rate (four times higher). (Smeets et al., 2017) observed that a strain rate of 2 %/s minimized the viscoelastic effects during static failure.

With reference to the mechanical characterization of FL, most of the analysed works stretched the samples up to failure, while few works focused on other aspects, as (Otsuka et al., 2020, 2018), where cycles of loading and unloading were performed also to quantify the hysteresis of the samples, and (Steinke et al., 2012), in which the interest was mainly on the linear elastic part of the curve and the influence of the experimental test setup. In (Bonaldi et al., 2023a) stress-relaxation tests were even performed, to study the viscoelastic properties of the tissue, while in (Aurora et al., 2011) a different stress distribution was analysed thanks to a biaxial setup. If failure was reached, the rupture should happen in the almost central part of the sample; on the contrary, a breakage close to the grips or the attachments points of the sample could highlight possible issues related to the sample mounting or preparation (Crawford, 1969). Indeed, variations among rupture locations could be potentially influenced also by the fibres directions.

3.2.3. Effectiveness of mechanical testing

Focussing on the strength, only few works analysed the ultimate tensile stress (UTS) (Balsly et al., 2008; Bonaldi et al., 2023a; Erivan et al., 2018; Hammer et al., 2012; Manon et al., 2022; Zwirner et al., 2019), but results appear to be not always comparable (Fig. 3a): indeed (Zwirner et al., 2019) reported the strength of ITT equal to 29.0 ± 17.0 MPa as a mean value, while (Manon et al., 2022) referred to a UTS of 96.8 ± 3.2 MPa, but also differentiated between the genders, while (Hammer et al., 2012) did not differ between female and male subjects, but the mean value (35.9 ± 16.4 MPa) was obtained from a specific age-range donors (19–44 y/o).

Bonaldi et al., (Bonaldi et al., 2023a) observed a strong anisotropy if adopting as loading direction the main fibres orientation of one layer with respect to the other, while (Erivan et al., 2018) observed a strength of 26.2 ± 14.5 MPa for FL without treatments and, testing the influence of different preservation methods, they found no significant difference between dry cryopreserved and freeze-dried samples; on the contrary, dimethylsulfoxide (DMSO) solution or gamma radiation were observed to alter biomechanical properties. Only (Balsly et al., 2008) showed a greater strength, equal to 93.4 ± 28.2 MPa, which deviates from the other results, but still in the range for that kind of biological tissue. One hypothetic reason could be a higher test velocity to perform the failure, which could have slightly stiffened the material, as well as the different conservation methods.

Among the considered articles, it has been found that the ultimate strain at break of human FL can vary between 3.5 % (Thomas et al., 1998) up to 19 % (Bonaldi et al., 2023a) in different scenarios (Fig. 3c). Indeed, also the strain may depend on many factors as use of steroids in donor clinical history (Thomas et al., 1998), fibres direction orientation (Bonaldi et al., 2023a), age and even height (Hammer et al., 2012; Zwirner et al., 2019), thus for these reasons its variation is quite broad.

As it was stated in the previous, the human FL is characterized by a globally non-linear stress–strain response, mainly due to the presence of collagen fibres, which strongly influence its mechanical behaviour. By considering the strain range between on average 2 and 5 % (Bonaldi et al., 2023a; Derwin et al., 2008; Hammer et al., 2012; Steinke et al., 2012)(Hammer et al., 2012; Steinke et al., 2012), the stress–strain curve appears quasi-linear and a value of E can be extracted, usually by linear fit of the curve slope, as reported in Table 3 and illustrated in Fig. 3d. Other authors preferred to consider the stress range, and the linear part was found between 4 and 11 MPa (Hammer et al., 2012; Steinke et al., 2012). In particular, the influence of the fibres directions, which provides this tissue with strong anisotropy, was explored by (Otsuka et al., 2018), who studied the mechanical response of human FL when stretched parallel to the fibres and along the transversal direction of anterior, lateral, medial and posterior thigh compartments, with reference to both genders. A clear difference in the mechanical response was observed, between directions (up to two orders of magnitude of variation between parallel and transverse direction) and also among the sites, revealing the lateral one as the stiffest one with the strongest anisotropy. However it should be noticed that the authors tested formaline-fixed samples, that, as investigated by (Steinke et al., 2012), it is a treatment that may stiffen the specimens with respect to fresh-frozen tissue, due to the formation of irreversible cross-links between the amino groups of the collagen. Indeed (Steinke et al., 2012) observed no statistical differences between fresh and formaline-rinced samples, thus concluding that this latter solution might also provide acceptable data for the elastic modulus of the FL. Despite the absolute values obtained in (Otsuka et al., 2018), Otsuka et al. threw a spotlight on the peculiar link between fibres orientation and tissue performance, as also demonstrated in the recent work by Bonaldi et al., (Bonaldi et al., 2023a) where differences were also observed between the mechanical behaviour of the two parallel connective layers which form the FL. In particular, from the failure tests, results suggested that the two parallel layers (Fig. 2c) contribute differently with reference to tissue strength, being characterized by a different tensile stiffness (Fig. 3a, results by (Bonaldi et al., 2023a)). These insights were supported by the different functional roles played by the two layers, since one the connection of the knee-hip axis or the adaptation to the muscular contraction. These difference may be observed also for the UTS (Fig. 3b), but minimal variations were found for the strain at break of the FL even if different loading directions were considered (Fig. 3c) (Bonaldi et al., 2023a).

When considering other features that could influence the FL biomechanics, a work by Otsuka et al. (Otsuka et al., 2020) pointed out a not negligeable variability of the mechanical properties along the ITT by analysing five different sites. Results highlighted a decrease in the elastic modulus from proximal to distal, suggesting that the tissue appear more compliant at the distal (patella) than other regions. In the study by Zwirner et al. (Zwirner et al., 2019), the elastic modulus appeared to be also influenced by gender, being correlated with height (for males), either with weight (for females). Additional alterations could be caused by other treatments and conservation (Steinke et al., 2012), but also hydration and adopted strain rate during the tests, resulting in a wide variability among authors, especially due to different protocols. Each

Table 3
Details of the evaluation process of the elastic (or Young's) modulus among the authors and stress or strain range considered on average (when reported).

Authors	Elastic modulus calculation		
	Method	Range	Comments
Balsly, C. L. et al. 2008	BlueHill software (Instron, Norwood, MA)	N/A	
Bonaldi L. et al. 2023	Linear fit with a custom Matlab script (Matlab 2021b, MathWorks)	3–6 % strain on average	
de Campos Azevedo, C. I. et al. 2021	Bilinear curve fit with a custom Matlab script (Matlab, MathWorks)	N/A	Obtained from the average stiffness of the linear region in each of the last 3 cycles of loading–unloading
Derwin, K. A. et al. 2008	Slope of the stress–strain curves in the linear region	2–5 % strain	
Erivan, R. et al. 2018	Software of the traction device (MTS 20 M)	N/A	
Hammer, N. et al. 2012	Secant stiffness in a constant range	4–11 MPa stress	
Manon, J. et al. 2022	Slope of the regression line in the linear region of the stress–strain curve	N/A	Obtained from the loading curves at two different velocities
Otsuka, S. et al. 2018	Slope of the regression line in the linear region of the stress–strain curve	N/A	
Otsuka, S. et al. 2020	Slope of the linear region of strain–stress curve (regression line)	N/A	
Smeets, K. et al. 2017	Slope of the regression line in the linear region of the stress–strain curve	N/A	
Steinke, H. et al. 2012	Secant of the linear part of the stress–strain curve	4–11 MPa stress	
Zwirner, J. et al. 2019	Regression in the linear slope of the nominal stress–strain curve	N/A	The linear elastic response of each sample was evaluated in the final load cycle, after preconditioning and until material failure

authors' results are reported in Table 2 and the variability is stressed in Fig. 3a, with values for E ranking from 1 to 500 MPa, with a few exceptions (especially for (Manon et al., 2022) where a value around 1500 MPa has been found). This being the case, FL appears to be well known from a clinical point of view, but its several biomechanical aspects still under identification.

As biological soft tissue, FL has been shown to exhibit viscoelasticity. Viscoelasticity is related to the remodelling process of the extracellular matrix, and to the proper orientation of the collagen fibres. During stress relaxation tests, stress decay for a time interval of 100 s–300 s has been observed (Bonaldi et al., 2023a; Chaudhry et al., 2007). Bonaldi et al. (Bonaldi et al., 2023a) were the first authors that investigated the viscoelastic properties of human FL, observing on average a stress relaxation of about 60 %, independently of loading directions, thus anisotropy seemed to not affect the viscous properties of this connective tissue (as also confirmed for the superficial fascia (Berardo et al., 2024)). The stress reduction after 300 s for the FL resulted greater with respect to other fascial tissues such as crural fascia (Stecco et al., 2014).

Moreover, also cycling loading protocols can be used as an indicator of the tissue viscoelasticity, simulating the physiological daily-living activities as well as the rehabilitation process. Indeed, (Ferro et al., 2015) performed dynamic tests (600 cycles) on tubularized ITT grafts and evinced that their elongations increased almost proportionally with increasing maximum load (from 50 N to 300 N of applied load, a displacement of 0.68–4.65 mm was measured, respectively). Wytrykowski et al. and Taylan et al. realized comparisons between the dynamic behavior of ITT grafts with respect to the gracilis (Taylan et al., 2022; Wytrykowski et al., 2016). In particular, the first tested ITT samples by adopting a 100 cycles protocol (0.5 Hz uniaxial tensile test up to 200 N), then up to failure, resulting in almost comparable maximum load and elongation between the two tissues. Meanwhile, Taylan et al. (Taylan et al., 2022) with a different protocol (200 cycles loading–unloading at 1 Hz followed by a creep test of 10 N/s up to 12 MPa for 100 s) reported the evidence that ITT showed a higher tissue hysteresis with respect to gracilis that means consequent higher heat damage and energy dissipation, while higher dynamic creep for ITT (of 0.7 ± 0.2 MPa) revealed tissue attitude to deform permanently.

4. Conclusions

The identification of possible biases that could lead to misleading of the results concerning the biomechanical properties of the human FL and related testing protocols have been presented. Considering the influences of material (e.g., donors, harvesting, cutting into strips), methods (e.g., protocols), mother nature (e.g., storage, thawing, hydration), operator and measure (e.g., manual measurements), machine set up (e.g., gripping system) in comparing literature works, the variability of the results highlighted the importance of defining a good practice for design, implementation and interpretation of experimental results (as example, current review tables could be used as checklist for tests management as well as literature articles analysis and comparison).

From a clinical point of view, the peculiar properties of the FL have made this tissue suitable for grafting, and consequently thrown a spotlight on its biomechanical behaviour, that has been investigated by some authors along the years. In many works, the application of FL grafts as substitutes of human tissues appeared to be a well-known procedure, even if the biomechanical aspect of this tissue is often omitted nor considered. Indeed, the different biomechanical characteristics of the FL with respect to the harvesting site, the gender, and the directions of the fibres, would require the definition of surgical protocols that guide its application in accordance with the biomechanical properties of FL as a multi-layered structure. Being an anisotropic and viscoelastic composite material, its response was observed to be influenced especially by its micro and macrostructure. Moreover, the mechanical properties of human FL could be altered by other factors, such as conservation, testing procedure, hydration and setup that sometimes appear to be a missing

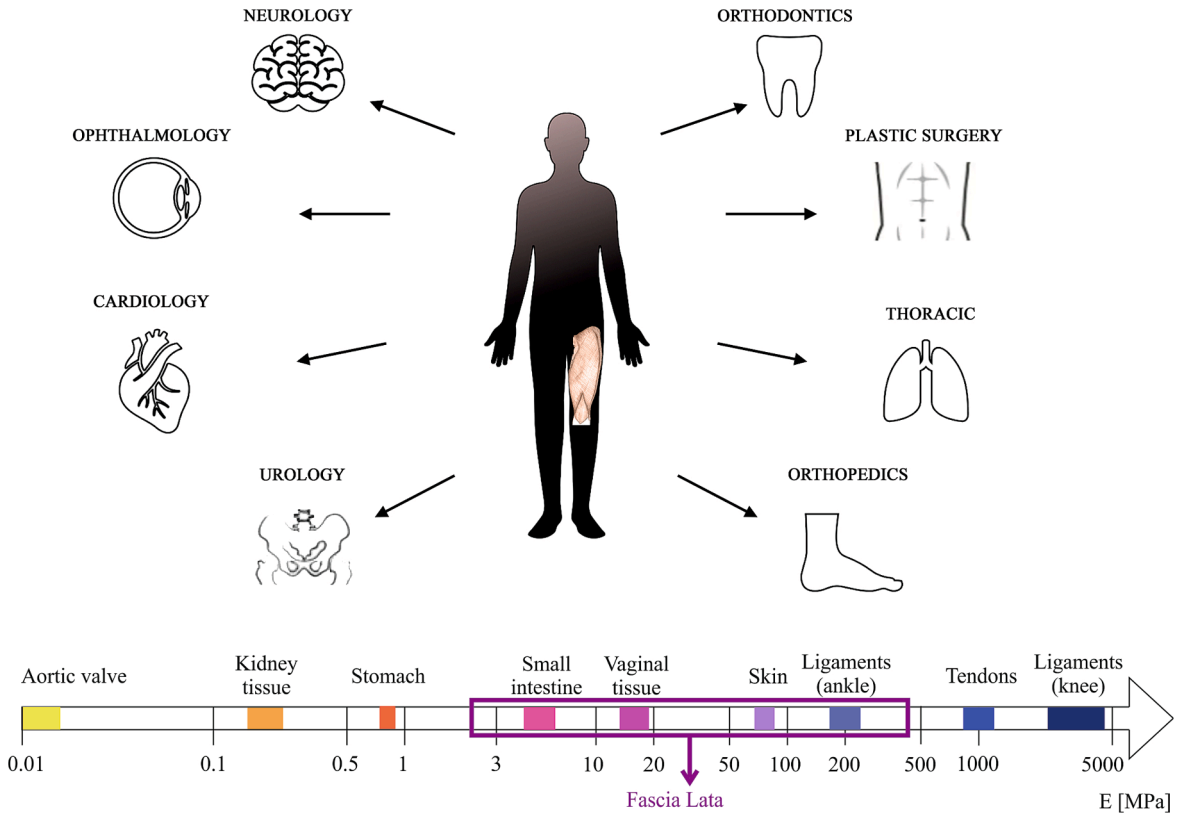

Fig. 4. Examples of application of FL auto- and allografts for surgical reconstruction from literature, with reference to Elastic Moduli of human soft tissues (reference values taken from (Singh and Chanda, 2021)).

information, even if this variability could result in a different biomechanical behaviour of the resultant construct graft.

Indeed, in many surgical procedures, the main focus is usually the thickness of FL grafts during strips preparation, since FL in the distal direction is thicker than proximal ones (de Campos Azevedo et al., 2021; Khiami et al., 2013), but no mechanical parameters, such as the UTS or *E*, are usually considered. In Fig. 4 it has been reported *E* of FL as found from the literature analysis with reference to various human soft tissues (Singh and Chanda, 2021) to highlight the most suitable fields of applications. Until now, only a few works reported the development of a novel reinforced fascia patch considering also fibres orientation to require adequate stiffness properties in accordance with the different directions (Aurora et al., 2011). An in-depth discussion on these topics may guide surgeons in the choice of the optimal location, harvesting technique and type of graft design, as well as in the development of synthetic or tissue-engineered alternatives. The characterization of graft properties for the comparison between different clinical treatments and their use in biomechanical models (Gordon et al., 2017) are both key requirements for risk assessment. Moreover, the biomechanical characterization of the fascia lata tissue, through experimental tests, is a milestone towards its in-vivo (i.e., though bioimaging (Bonaldi et al., 2023c)) and in-silico characterization. Within this review a collection of those features that could affect the mechanical properties and behaviour of human FL were analysed, in order to provide the reader with a clear overview of all the aspects that should be considered when planning a mechanical test for FL autograft or allograft. All these insights would contribute to improve the biomechanical knowledge of FL and thus optimize graft applications for tuneable surgical and rehabilitation practices towards an effective personalised medicine.

5. Ethics approval and consent to participate

Not applicable.

6. Consent for publication

Not applicable.

7. Funding sources

This work was supported by MIUR, FISR 2019, Project n° FISR2019_03221, titled CECOMES: CEntro di studi sperimentali e COmputazionali per la ModElliStica applicata alla chirurgia.

CRediT authorship contribution statement

Lorenza Bonaldi: Writing – review & editing, Writing – original draft, Investigation, Formal analysis, Data curation, Conceptualization. **Chiara Giulia Fontanella:** Writing – review & editing, Writing – original draft, Supervision, Funding acquisition, Conceptualization. **Carla Stecco:** Writing – review & editing, Writing – original draft, Conceptualization. **Alice Berardo:** Writing – review & editing, Writing – original draft, Investigation, Formal analysis, Data curation, Conceptualization.

Declaration of competing interest

The authors declare that they have no known competing financial interests or personal relationships that could have appeared to influence the work reported in this paper.

Acknowledgements

The authors have no specific acknowledgements to address.

References

Aurora, A., Mesiha, M., Tan, C.D., Walker, E., Sahoo, S., Iannotti, J.P., McCarron, J.A., Derwin, K.A., 2011. Mechanical characterization and biocompatibility of a novel reinforced fascia patch for rotator cuff repair. J. Biomed. Mater. Res. - Part A 99 A, 221–230. https://doi.org/10.1002/jbm.a.33179.

Balsly, C.R., Cotter, A.T., Williams, L.A., Gaskins, B.D., Moore, M.A., Wolfinbarger, L., 2008. Effect of low dose and moderate dose gamma irradiation on the mechanical properties of bone and soft tissue allografts. Cell Tissue Bank. 9, 289–298. https://doi.org/10.1007/s10561-008-9069-0.

Benetazzo, L., Bizzego, A., De Caro, R., Frigo, G., Guidolin, D., Stecco, C., 2011. 3D reconstruction of the crural and thoracolumbar fasciae. Surg. Radiol. Anat. 33, 855–862. https://doi.org/10.1007/s00276-010-0757-7.

Benjamin, M., 2009. The fascia of the limbs and back - a review. J. Anat. 214, 1–18. https://doi.org/10.1111/j.1469-7580.2008.01011.x.

Berardo, A., Bonaldi, L., Stecco, C., Fontanella, C.G., 2024. Biomechanical properties of the human superficial fascia: Site-specific variability and anisotropy of abdominal and thoracic regions. J. Mech. Behav. Biomed. Mater. 157, 106637. https://doi.org/10.1016/j.jmbbm.2024.106637.

Birnbaum, K., Siebert, C.H., Pandorf, T., Schopphoff, E., Prescher, A., Niethard, F.U., 2004. Anatomical and biomechanical investigations of the iliotibial tract. Surg. Radiol. Anat. 26, 433–446. https://doi.org/10.1007/s00276-004-0265-8.

Bonaldi, L., Berardo, A., Pirri, C., Stecco, C., Carniel, E.L., Fontanella, C.G., 2023a. Mechanical Characterization of Human Fascia Lata: Uniaxial Tensile Tests from Fresh-Frozen Cadaver Samples and Constitutive Modelling 1–13. doi: 10.3390/bioengineering10020226.

Bonaldi, L., Fontanella, C.G., Pirri, C., Stecco, C., Berardo, A., 2023b. The biomechanical behaviour of fascial system: Superficial VS Deep Fascia, in: Convegno Nazionale Di Bioingegneria. Patron Editore S.r.l.

Bonaldi, L., Pretto, A., Pirri, C., Uccheddu, F., Fontanella, C.G., Stecco, C., 2023c. Deep learning-based medical images segmentation of musculoskeletal anatomical structures: a survey of bottlenecks and strategies. Bioengineering 10, 137. https://doi.org/10.3390/bioengineering10020137.

Brown, S.L., Govier, F.E., Morgan, T.O., O'Connell, H.E., 2000. Cadaveric versus autologous fascia lata for the pubovaginal sling: Surgical outcome and patient satisfaction. J. Urol. 164, 1633–1637. https://doi.org/10.1016/S0022-5347(05)67046-2.

Butler, D.L., Grood, E.S., Noyes, F.R., Zernicke, R.F., Brackett, K., 1984. Effects of structure and strain measurement technique on the material properties of young human tendons and fascia. J. Biomech. 17, 579–596. https://doi.org/10.1016/0021-9290(84)90090-3.

Caplan, N., Kader, D.F., 2014. Biomechanical Analysis of Human Ligament Grafts Used in Knee-Ligament Repairs and Reconstructions. In: Classic Papers in Orthopaedics. Springer London, London, pp. 145–147. doi: 10.1007/978-1-4471-5451-8_35.

Chaudhry, H., Huang, C.Y., Schleip, R., Ji, Z., Bukiet, B., Findley, T., 2007. Viscoelastic behavior of human fasciae under extension in manual therapy. J. Bodyw. Mov. Ther. 11, 159–167. https://doi.org/10.1016/j.jbmt.2006.08.012.

Cheng, S., Clarke, E.C., Bilston, L.E., 2009. The effects of preconditioning strain on measured tissue properties. J. Biomech. 42, 1360–1362. https://doi.org/10.1016/j.jbiomech.2009.03.023.

Choe, J.M., Kothandapani, R., James, L., Bowling, D., 2001. Autologous, cadaveric, and synthetic materials used in sling surgery: comparative biomechanical analysis. Urology 58, 482–486. https://doi.org/10.1016/S0090-4295(01)01205-5.

Crawford, J.S., 1969. Nature of fascia lata and its fate after implantation. Am. J. Ophthalmol. 67, 900–907. https://doi.org/10.1016/0002-9394(69)90084-1.

de Campos Azevedo, C.I., Leiria Pires Gago Ângelo, A.C., Quental, C., Gonçalves, S., Folgado, J., Ferreira, N., Sevivas, N., 2021. Proximal and mid-thigh fascia lata graft constructs used for arthroscopic superior capsule reconstruction show equivalent biomechanical properties: an in vitro human cadaver study. JSES Int. 5, 439–446. https://doi.org/10.1016/j.jseint.2021.01.016.

Derwin, K.A., Baker, A.R., Spragg, R.K., Leigh, D.R., Farhat, W., Iannotti, J.P., 2008. Regional variability, processing methods, and biophysical properties of human fascia lata extracellular matrix. J. Biomed. Mater. Res. Part A 84A, 500–507. https://doi.org/10.1002/jbm.a.31455.

Ding, S., Ge, Y., Zheng, M., Ding, W., Jin, W., Li, J., Chen, S., 2019. Arthroscopic superior capsular reconstruction using "sandwich" patch technique for irreparable rotator cuff tears. Arthrosc. Tech. 8, e953–e959. https://doi.org/10.1016/j.eats.2019.05.004.

Dwyer, N.T., Kreder, K.J., 2008. Fascia Lata Sling, third ed., Female Urology. Elsevier Inc. doi: 10.1016/B978-1-4160-2339-5.50087-2.

Ebrahimi, M., Mohammadi, A., Ristaniemi, A., Stenroth, L., Korhonen, R.K., 2019. The effect of different preconditioning protocols on repeatability of bovine ACL stress-relaxation response in tension. J. Mech. Behav. Biomed. Mater. 90, 493–501. https://doi.org/10.1016/j.jmbbm.2018.10.041.

Erivan, R., Aubret, S., Villatte, G., Cueff, R., Mulliez, A., Descamps, S., Boisgard, S., 2018. Irradiation at 11 kGy conserves the biomechanical properties of fascia lata better than irradiation at 25 kGy. Clin. Biomech. 60, 100–107. https://doi.org/10.1016/j.clinbiomech.2018.10.016.

Ferro, F.P., Philippon, M.J., Rasmussen, M.T., Smith, S.D., Laprade, R.F., Wijdicks, C.A., 2015. Tensile properties of the human acetabular labrum and hip labral reconstruction grafts. Am. J. Sports Med. 43, 1222–1227. https://doi.org/10.1177/0363546514568086.

Flanagan, J.C., Campbell, C.B., 1981. The use of autogenous fascia lata to correct lid and orbital deformities. Trans. Am. Ophthalmol. Soc. 79, 227–242.

Gordon, K., Brett, A., Weber, J.F., 2017. Uniaxial Biomechanical Testing of Ligaments and Tendons, Experimental Methods in Orthopaedic Biomechanics. Elsevier Inc. doi: 10.1016/B978-0-12-803802-4.00022-6.

Gratz, C.M.M., 1931. Tensile strength and elasticity tests on human fascia lata. J. Bone Jt. Surg.

Hammer, N., Lingslebe, U., Aust, G., Milani, T.L., Hädrich, C., Steinke, H., 2012. Ultimate stress and age-dependent deformation characteristics of the iliotibial tract. J. Mech. Behav. Biomed. Mater. 16, 81–86. https://doi.org/10.1016/j.jmbbm.2012.04.025.

Ionescu, M.I., Ross, D.N., Deac, R.C., Wooler, G.H., 1970. Heart valve replacement with autologous fascia lata. J. Thorac. Cardiovasc. Surg. 60, 331–354. https://doi.org/10.1016/s0022-5223(19)42347-7.

Ionescu, M.I., Pakrashi, B.C., Holden, M.P., Mary, D.A., Wooler, G.H., 1972. Results of aortic valve replacement with frame-supported fascia lata and pericardial grafts. J. Thorac. Cardiovasc. Surg. 64, 340–353. https://doi.org/10.1016/s0022-5223(19)39830-7.

Khiami, F., Wajsfisz, A., Meyer, A., Rolland, E., Catonné, Y., Sariali, E., 2013. Anterior cruciate ligament reconstruction with fascia lata using a minimally invasive arthroscopic harvesting technique. Orthop. Traumatol. Surg. Res. 99, 99–105. https://doi.org/10.1016/j.otsr.2012.09.017.

Kubricht, W.S., Williams, B.J., Eastham, J.A., Venable, D.D., 2001. Tensile strength of cadaveric fascia lata compared to small intestinal submucosa using suture pull through analysis. J. Urol. 165, 486–490. https://doi.org/10.1097/00005392-200102000-00031.

Lemer, M.L., Chaikin, D.C., Blaivas, J.G., 1999. Tissue strength analysis of autologous and cadaveric allografts for the pubovaginal sling. Neurourol. Urodyn. 18, 497–503. https://doi.org/10.1002/(SICI)1520-6777(1999)18:5<497::AID-NAU12>3.0.CO;2-K.

Manon, J., Evrard, R., Maistriaux, L., Fievé, L., Heller, U., Magnin, D., Boisson, J., Kadlub, N., Schubert, T., Lengelé, B., Behets, C., Cornu, O., 2022. Periosteum and fascia lata: Are they so different? Front. Bioeng. Biotechnol. 10, 1–16. https://doi.org/10.3389/fbioe.2022.944828.

McCarron, J.A., Milks, R.A., Mesiha, M., Aurora, A., Walker, E., Iannotti, J.P., Derwin, K. A., 2012. Reinforced fascia patch limits cyclic gapping of rotator cuff repairs in a human cadaveric model. J. Shoulder Elb. Surg. 21, 1680–1686. https://doi.org/10.1016/j.jse.2011.11.039.

McEnany, M.T., Ross, D.N., Yates, A.K., 1972. Valve failure in seventy-two frame-supported autologous fascia lata mitral valves. Two-Year Follow-up. J. Thorac. Cardiovasc. Surg. 63, 199–214. https://doi.org/10.1016/s0022-5223(19)41928-4.

Milks, R.A., Kolmodin, J.D., Ricchetti, E.T., Iannotti, J.P., Derwin, K.A., 2018. Augmentation with a reinforced acellular fascia lata strip graft limits cyclic gapping of supraspinatus repairs in a human cadaveric model. J. Shoulder Elb. Surg. 27, 1105–1111. https://doi.org/10.1016/j.jse.2017.12.016.

Molnar, T.F., Rendeki, S., Lukacs, L., Horvath, O.P., 2003. Improvement of air tightness of stapled lung parenchyma using fascia lata. Interact. Cardiovasc. Thorac. Surg. 2, 503–505.

Otsuka, S., Yakura, T., Ohmichi, Y., Ohmichi, M., Naito, M., Nakano, T., Kawakami, Y., 2018. Site specificity of mechanical and structural properties of human fascia lata and their gender differences: a cadaveric study. J. Biomech. 77, 69–75. https://doi.org/10.1016/j.jbiomech.2018.06.018.

Otsuka, S., Shan, X., Kawakami, Y., 2019. Dependence of muscle and deep fascia stiffness on the contraction levels of the quadriceps: An in vivo supersonic shear-imaging study. J. Electromyogr. Kinesiol. 45, 33–40. https://doi.org/10.1016/j.jelekin.2019.02.003.

Otsuka, S., Shan, X., Yoshida, K., Yakura, T., Naito, M., Kawakami, Y., 2020. Site dependent elastic property of human iliotibial band and the effect of hip and knee joint angle configuration. J. Biomech. 109, 109919. https://doi.org/10.1016/j.jbiomech.2020.109919.

Pirri, C., Fede, C., Petrelli, L., Guidolin, D., Fan, C., De Caro, R., Stecco, C., 2022. Elastic Fibres in the subcutaneous tissue: Is there a difference between superficial and muscular fascia? A cadaver study. Ski. Res. Technol. 28, 21–27. https://doi.org/10.1111/srt.13084.

Platzer, W., Orlandini, G., Spitzer, G., 2014. Anatomia umana: Apparato locomotore / Werner Platzer ; disegni di Gerhard Spitzer, Atlante tascabile di anatomia umana. Casa Editrice Ambrosiana.

Polacek, M., 2019. Arthroscopic superior capsular reconstruction with acellular porcine dermal xenograft for the treatment of massive irreparable rotator cuff tears. Arthrosc. Sport. Med. Rehabil. 1, e75–e84. https://doi.org/10.1016/j.asmr.2019.08.001.

Powell, C.R., Simsiman, A.J., Menefee, S.A., 2004. Anterior vaginal wall hammock with fascia lata for the correction of stage 2 or greater anterior vaginal compartment relaxation. J. Urol. 171, 264–267. https://doi.org/10.1097/01.ju.0000100260.36697.91.

Singh, G., Chanda, A., 2021. Mechanical properties of whole-body soft human tissues: A review. Biomed. Mater. 16. https://doi.org/10.1088/1748-605X/ac2b7a.

Smeets, K., Bellemans, J., Scheys, L., Eijnde, B.O., Slane, J., Claes, S., 2017. Mechanical analysis of extra-articular knee ligaments. part two: tendon grafts used for knee ligament reconstruction. Knee 24, 957–964. https://doi.org/10.1016/j.knee.2017.07.011.

Stecco, A., Macchi, V., Stecco, C., Porzionato, A., Ann Day, J., Delmas, V., De Caro, R., 2009a. Anatomical study of myofascial continuity in the anterior region of the upper limb. J. Bodyw. Mov. Ther. 13, 53–62. https://doi.org/10.1016/j.jbmt.2007.04.009.

Stecco, A., Gilliar, W., Hill, R., Brad, F., Stecco, C., 2013. The anatomical and functional relation between gluteus maximus and fascia lata. J. Bodyw. Mov. Ther. 17, 512–517. https://doi.org/10.1016/j.jbmt.2013.04.004.

Stecco, A., Bonaldi, L., Fontanella, C.G., Stecco, C., Pirri, C., 2023. The effect of mechanical stress on hyaluronan fragments' inflammatory cascade: clinical implications. Life 13, 2277. https://doi.org/10.3390/life13122277.

Stecco, C., Porzionato, A., Lancerotto, L., Stecco, A., Macchi, V., Ann Day, J., De Caro, R., 2008. Histological study of the deep fasciae of the limbs. J. Bodyw. Mov. Ther. 12, 225–230. https://doi.org/10.1016/j.jbmt.2008.04.041.

Stecco, C., Pavan, P.G., Porzionato, A., Macchi, V., Lancerotto, L., Carniel, E.L., Natali, A. N., De Caro, R., 2009b. Mechanics of crural fascia: from anatomy to constitutive modelling. Surg. Radiol. Anat. 31, 523–529. https://doi.org/10.1007/s00276-009-0474-2.

Stecco, C., Pavan, P., Pachera, P., De Caro, R., Natali, A., 2014. Investigation of the mechanical properties of the human crural fascia and their possible clinical implications. Surg. Radiol. Anat. 36, 25–32. https://doi.org/10.1007/s00276-013-1152-y.

Stecco, C., Schleip, R., 2016. A fascia and the fascial system. J. Bodyw. Mov. Ther. 20, 139–140. https://doi.org/10.1016/j.jbmt.2015.11.012.

Stecco, C., 2014. Functional Atlas of the human Fascial system.

Steinke, H., Lingslebe, U., Böhme, J., Slowik, V., Shim, V., Hädrich, C., Hammer, N., 2012. Deformation behavior of the iliotibial tract under different states of fixation. Med. Eng. Phys. 34, 1221–1227. https://doi.org/10.1016/j.medengphy.2011.12.009.

Szotek, S., Czogała, J., Ścigała, K., Marycz, K., Maksymowicz, K., 2012. The biomechanical and ultrastructural properties of human fascia lata. J. Bodyw. Mov. Ther. 16, 397–398. https://doi.org/10.1016/j.jbmt.2012.01.036.

Takahashi, Y., Leibovitch, I., Kakizaki, H., 2015. Frontalis suspension surgery in upper eyelid blepharoptosis. Open Ophthalmol. J. 4, 91–97. https://doi.org/10.2174/1874364101004010091.

Taylan, O., Slane, J., van Beek, N., Dandois, F., Scheys, L., Claes, S., 2022. Characterizing the viscoelastic properties of the anterolateral ligament and grafts commonly used in its reconstruction. SSRN Electron. J. 104, 1–8. https://doi.org/10.2139/ssrn.4251170.

Thomas, O.L., Morrison, C., Howard, L., Oni, O.O.A., 1998. The biomechanical properties of fascia lata grafts: a preliminary study. Injury 29, 227–228. https://doi.org/10.1016/S0020-1383(97)00192-7.

Turnipseed, W.D., Hurschler, C., Vanderby, R., 1995. The effects of elevated compartment pressure on tibial arteriovenous flow and relationship of mechanical and biochemical characteristics of fascia to genesis of chronic anterior compartment syndrome. J. Vasc. Surg. 21, 810–817. https://doi.org/10.1016/S0741-5214(05)80012-6.

Wood Jones, F., 1944. Structure and function as seen in the foot. Postgrad. Med. J. 20, 330. https://doi.org/10.1136/pgmj.20.228.330.

Wytrykowski, K., Swider, P., Reina, N., Murgier, J., Laffosse, J.M., Chiron, P., Cavaignac, E., 2016. Cadaveric study comparing the biomechanical properties of grafts used for knee anterolateral ligament reconstruction. Arthrosc. - J. Arthrosc. Relat. Surg. 32, 2288–2294. https://doi.org/10.1016/j.arthro.2016.03.004.

Zwirner, J., Babian, C., Ondruschka, B., Schleifenbaum, S., Scholze, M., Waddell, N.J., Hammer, N., 2019. Tensile properties of the human iliotibial tract depend on height and weight. Med. Eng. Phys. 69, 85–91. https://doi.org/10.1016/j.medengphy.2019.05.001.